AMACO is a novel component of the basement membrane associated Fraser complex

Rebecca J. Richardson[1,2,*], Jan M. Gebauer[3], Jin-Li Zhang[1,2,#], Birgit Kobbe[3], Douglas R. Keene[4], Kristina Røkenes Karlsen[5], Stefânia Richetti[1], Alexander P. Wohl[3], Gerhard Sengle[3], Wolfram F. Neiss[5], Mats Paulsson[2,3,6], Matthias Hammerschmidt[1,2,6,§], and Raimund Wagener[2,3,§]

[1]Institute of Developmental Biology, University of Cologne, Cologne, Germany

[2]Center for Molecular Medicine Cologne, Medical Faculty, University of Cologne, Cologne, Germany

[3]Center for Biochemistry, University of Cologne, Cologne, Germany

[4]Microimaging Center, Shriners Hospital for Children, Portland, Oregon, USA

[5]Department of Anatomy I, Medical Faculty, University of Cologne, Cologne, Germany

[6]Cologne Excellence Cluster on Cellular Stress Responses in Aging-Associated Diseases, University of Cologne, Cologne, Germany

* Current address: Departments of Physiology and Biochemistry, School of Medical Sciences, Bristol, UK

Current address: Department of Chemistry and Biochemistry, University of Montana, Missoula, USA

§ Authors for correspondence:

Raimund Wagener, Institute for Biochemistry II, Medical Faculty, University of Cologne, Joseph-Stelzmann-Str. 52, D-50931 Cologne, Germany, Tel.: +49 221 478 6990; Fax: +49 221 478 6977, E-Mail: raimund.wagener@uni-koeln.de

Matthias Hammerschmidt, Institute of Developmental Biology, Biocenter, University of Cologne, Zülpicher Str. 47b, D-50674 Cologne, Tel.: +49 221 470 5665; Fax: +49 221 470 5164, E-mail: mhammers@uni-koeln.de

Short title: AMACO is a mediator of the Fraser complex

Abbreviations: FS, Fraser syndrome; BM, basement membrane; BNAR, bifid nose, renal agenesis, and anorectal malformations syndrome; MOTA, Manitoba-oculo-tricho-anal syndrome; RU, response unit; TEM, transmission electron microscopy.

Abstract

Fraser syndrome (FS) is a phenotypically variable, autosomal recessive disorder characterized by cryptophthalmus, cutaneous syndactyly and other malformations resulting from mutations in *FRAS1*, *FREM2* and *GRIP1*. Transient embryonic epidermal blistering causes the characteristic defects of the disorder. Fras1, Frem1 and Frem2 form the extracellular Fraser complex, which is believed to stabilize the basement membrane (BM). However, several cases of FS could not be attributed to mutations in *FRAS1*, *FREM2* or *GRIP1*, suggesting there is an additional genetic contribution to this disorder. AMACO, encoded by the *VWA2* gene, has a very similar tissue distribution to the Fraser complex proteins. In mouse, AMACO is expressed in the developing lungs, kidney and skin where it is closely associated with the BM. In zebrafish AMACO is also associated with BMs, particularly in the developing fins, somite borders and the craniofacial region. Here, we show that AMACO deposition is lost in Fras1 deficient zebrafish and mice and that Fras1 and AMACO interact directly via their CSPG and P2 domains. Knockdown of *vwa2*, which alone causes no phenotype, enhances the phenotype of hypomorphic Fras1 mutant zebrafish. Together, our data suggest that AMACO represents a novel member of the Fraser complex.

Introduction

Fraser syndrome (FS; OMIM #219000) is a rare, autosomal recessive disorder characterized by cryptophthalmus, cutaneous syndactyly and variable other malformations (Slavotinek and Tifft, 2002). Both the human syndrome and the closely related bleb mouse phenotype are caused by mutations in genes encoding proteins of the Fraser complex, *FRAS1, FREM2* and, in mice, *Frem1* (McGregor *et al.*, 2003; Jadeja *et al.*, 2005). The ectodomain of Fras1, which is shed from the cell surface, forms a ternary complex with Frem1 and Frem2 which reciprocally stabilizes these at the BM. The proteins are characterized by the presence of 12 CSPG repeats and single or multiple Calx-β domain(s) (Kiyozumi *et al.*, 2007). In addition mutations in *GRIP1*, which encodes a cytoplasmic scaffolding protein, result in classical FS (Vogel *et al.*, 2012). Indeed, it has been described that one of the mouse skin bleb mutants results from a mutation in Grip1, that Grip1 binds directly to Fras1, and that it is required for Fras1 localization at the BM (Takamiya *et al.*, 2004; Long *et al.*, 2008). Analysis of the mouse bleb mutants revealed transient embryonic epidermal blistering, particularly over the developing eyes and digits, as the likely primary defect leading to the later malformations characteristic of the human disorder (McGregor *et al.*, 2003; Vrontou *et al.*, 2003; Jadeja *et al.*, 2005). The blisters result from a rupture just beneath the lamina densa of the BM and a separation of the dermis from the epidermis (McGregor *et al.*, 2003; Vrontou *et al.*, 2003; Jadeja *et al.*, 2005). Indeed, Fras1, Frem1 and Frem2 have been shown by immuno-gold EM to be localized on the dermal side of the lamina densa at islands normally associated with anchoring fibrils (Dalezios *et al.*, 2007; Petrou *et al.*, 2007a; Petrou *et al.*, 2007b). The Fraser complex associated protein, Frem3, has a similar ultrastructural localization although this expression is independent of Fras1 (Petrou *et al.*, 2007b).

Despite the identification of mutations in *FRAS1*, *FREM2* and *GRIP1* in both mice and humans with FS, a proportion of human cases remain unresolved suggesting that other genes may be involved (van Haelst *et al.*, 2008; Vogel *et al.*, 2012). Mutations in *FREM1* were recently shown to result in bifid nose, renal agenesis, and anorectal malformations (BNAR) and Manitoba-oculo-tricho-anal (MOTA) syndromes, two rare conditions with many similar phenotypic traits to FS, although milder (Alazami *et al.*, 2009; Slavotinek *et al.*, 2011). Recent analysis of ENU-induced mutants in zebrafish (*Danio rerio*) exhibiting transient blistering within the developing fins reveals functional conservation of the FS complex in lower vertebrates and suggests new potential FS-causing genes, such as *hemicentin1* (*hmcn1*), encoding a large extracellular matrix protein (Carney *et al.*, 2010) whose biochemical relationship to the FS complex is unclear.

Via a biochemical candidate approach in zebrafish and subsequent analysis in mice, we have identified a novel member of the Fraser complex, AMACO, encoded by the *VWA2* gene. AMACO (VWA2 protein) is a member of the von Willebrand factor A (VWA) domain containing protein superfamily (Whittaker and Hynes, 2002). The protein consists of an N-terminal VWA domain, which is followed by a cysteine-rich domain, an epidermal growth factor (EGF)-like domain carrying elongated O-glucosylated and O-fucosylated glycan chains and two more VWA domains. At the C-terminus another EGF-like domain and a unique domain are present (Sengle *et al.*, 2003; Gebauer *et al*., 2008). Analysis of mice and zebrafish revealed specific expression of AMACO at the BM of multiple tissues during development (Gebauer *et al.*, 2010; Gebauer *et al.*, 2009; Sengle *et al.*, 2003). We demonstrate that AMACO is lost from both zebrafish and mouse mutants that lack Fras1 expression and that Fras1 and AMACO interact directly. Finally, we show that targeted knockdown of AMACO in zebrafish, which produces no overt phenotype alone, enhances the phenotype severity of hypomorphic Fras1 mutant zebrafish suggesting a supportive role for AMACO in the Fraser complex.

Results

AMACO is reduced or absent in Fras1 mutant zebrafish

It was previously shown that AMACO is expressed during zebrafish development and exhibits a highly similar expression pattern to that of the FS genes, *fras1*, *frem1a*, *frem1b*, *frem2a*, *frem2b* and *frem3* (Carney *et al.*, 2010; Gebauer *et al.*, 2010). We, therefore, analyzed the expression of AMACO in our panel of Fraser complex and related mutants: *fras1*$^{te262/te262}$, *fras1*$^{tm95b/tm95b}$, *frem2a*$^{ta90/ta90}$, *frem1a*$^{tc280b/tc280b}$ and *hmcn1*$^{tq207/tq207}$ (Carney *et al.*, 2010). AMACO is strongly expressed in the myosepta, the extracellular boundaries between the somites, and the developing caudal fin of 32 hpf wild-type zebrafish (Figure 1a). This expression in the myosepta and caudal fin is very similar to that of Fras1 (Figure 1a, inset). AMACO expression, however, was completely lost in null *fras1*$^{te262/te262}$ fish (Figure 1b) and reduced in hypomorphic *fras1*$^{tm95b/tm95b}$ fish (Figure 1c) exactly correlating with Fras1 levels (Figure 1b and c, inset). By contrast, expression of AMACO was normal in *frem2a*$^{ta90/ta90}$, *frem1a*$^{tc280b/tc280b}$ and *hmcn1*$^{tq207/tq207}$ fish (Figure 1d-f). The expression level of Fras1 was also normal in each of these mutant lines (Figure 1d-f, inset). Quantification of immunoblots from whole zebrafish extracts confirmed the complete loss of AMACO in null *fras1*$^{te262/te262}$ fish and a strong reduction in hypomorphic *fras1*$^{tm95b/tm95b}$ fish. In the other mutants the level of AMACO remained normal or was only slightly reduced when compared to wild type levels. In situ hybridization and RT-PCR revealed that comparable levels of vwa2 mRNA are present in wild type and fras1 mutant fish (Suppl. 1), indicating that *vwa2* transcription is not affected.

AMACO is absent from *Fras1*$^{bl/bl}$ mice

Next, we analyzed the expression of AMACO in *Fras1*$^{bl/bl}$ mice. During mouse development AMACO is specifically localized at the BMs of skin, lung, heart, tooth germs and kidney (Sengle *et al.*, 2003). Analysis of these regions in E14.5 *Fras1*$^{bl/bl}$ mice revealed a complete loss of AMACO from the epidermal BM (Figure 2c) when compared to wild-type or *Fras1*$^{+/bl}$ littermates (Figure 2a-b) even though laminin deposition was normal (Figure 2d-f). Similarly, analysis of a blistered region over the eye of a *Fras1*$^{bl/bl}$ E14.5 embryo revealed a complete lack of AMACO expression (Figure 2g) even though laminin deposition demonstrated that a BM was still present as reported previously (Figure 2h; Vrontou *et al.*, 2003). Analysis of other regions, including the eyelid, kidney and developing tooth germs at E14.5 also revealed a complete loss of AMACO deposition (Figure 2i-l and data not shown).

AMACO and Fras1 co-localize beneath the lamina densa

Previous ultrastructural examinations demonstrated that Fras1, Frem1, Frem2 and AMACO are all localized at the BM zone (Gebauer *et al.*, 2009; Dalezios *et al.*, 2007; Petrou *et al.*, 2007a; Petrou *et al.*, 2007b). To determine co-localization of Fras1 and AMACO, double immunoelectron microscopy labeling was performed on P0 mouse skin using secondary antibodies coupled to different sized gold particles. Both proteins were detected in distinct regions, anchoring plaques, in the dermis close to the BM (Figure 3a and b). These AMACO and Fras1 positive patches often occurred where anchoring fibrils fuse (Figure 3a). Although regions were observed where only one protein was present, mostly AMACO and Fras1 co-localized (Figure 3a and b). Collagen VII/Fras1 double immunoelectron microscopy showed that collagen VII, a major component of anchoring fibrils, occurs in proximity to Fras1 at anchoring plaques, but mostly at the opposite side of the plaque indicating that the two proteins may not interact

directly (Figure 3c).

The AMACO fragment P2 binds to Fras1 CSPG repeats

To test for direct interactions between AMACO and the Fras1 ectodomain we employed surface plasmon resonance assays. For AMACO, we generated recombinant full-length protein as well as protein fragments corresponding to AMACO domains P1, P2 and P3 (Figure 4a). The recombinant expression of the full-length Fras1 ectodomain repeatedly failed (data not shown). To overcome this problem, Fras1 cDNA fragments, representing the VWC-, Furin-like-, CSPG-, and Calx-β domains and the unique domain alone (Figure 4a) were cloned for protein production, but only the Furin-like-, CSPG-, and Calx-β domains were well expressed.

Of these Fras1 fragments, we were only able to immobilize the CSPG domains on the sensor chip. When full-length AMACO was injected as soluble analyte at increasing concentrations (0–400 nM) over the CSPG chip we obtained association and dissociation curves (Figure 4b) which could be fitted with a Langmuir 1:1 binding model and could calculate a dissociation constant (K_D) of 75 nM. Of the three different domains (P1, P2, P3), binding to immobilized Fras1 CSPG was only seen with AMACO P2 (K_D 151 nM) (Figure 4b). This binding is independent of the two unusual glycan chains on AMACO P2, as mutant forms lacking either one or both glycosylation sites still bound to immobilized Fras1 CSPG with similar K_Ds between 77 and 108 nM (data not shown).

In the reverse set up (immobilization of AMACO P2 on the sensor chip and injection of the Fras1 CSPG), we could confirm the binding between the AMACO P2 domain and the Fras1 CSPG domain (K_D 42 nM; Figure 4c).

Loss of AMACO does not affect zebrafish development

To analyze the role of AMACO during zebrafish development, we generated two translation inhibiting morpholinos, which were injected into the yolk of fertilized eggs. Neither morpholino gave an obvious phenotype (Figure 5a-d) even though immunofluorescence analysis of the morphants clearly showed a strong decrease in AMACO protein detection levels (Figure 5c, d, inset). In particular, caudal fin development was normal (Figure 5a, b). In agreement, the expression of Fras1 in developing caudal fin and myosepta was normal in *vwa2* morphants (Figure 5c, d). Furthermore, knockdown of AMACO did not result in any obvious alteration in the structure of the pronephros and did not result in edema, which could indicate a failure in pronephros function (Drummond, 2005, data not shown). As AMACO is strongly expressed in the myosepta, potential ultrastructural changes in this region of the *vwa2* morphants were studied by transmission electron microscopy (TEM). However, analysis of wild-type and morphant embryos at 48 hpf revealed no obvious differences in the architecture of the myosepta or in the connection to the neighbouring myotomes (Figure 5e and f). All injected larvae developed normally and showed no obvious defects at 80 hpf in overall morphology, fin development or development of the facial skeleton, areas which are particularly affected in Fras1 mutant zebrafish (Carney *et al.*, 2010; Talbot *et al.*, 2012) (Figure 5g and h).

MO knockdown of AMACO in Fras1 hypomorphic zebrafish results in a more severe phenotype

The loss of AMACO in Fras1 deficient zebrafish and mice suggests that Fras1 is required for AMACO deposition or protein stability. To determine if AMACO stabilizes Fras1 protein at the

BM, we injected a *vwa2* specific MO into eggs resulting from an in-cross of *fras1*$^{+/tm95b}$ fish (Figure 6). These fish carry the missense mutation G3816W in Fras1 and exhibit reduced, but detectable levels of Fras1 protein (Figure 1c, Figure 6b) and are therefore believed to represent a hypomorphic allele. When an uninjected in-cross of *fras1*$^{+/tm95b}$ fish (n=415 (327=wt, 88=mut)) was compared to an in-cross of *fras1*$^{+/te262}$ (null allele) fish (n=88 (65=wt, 23=mut)), *fras1*$^{tm95b/tm95b}$ fish exhibit a milder caudal fin blistering phenotype as assessed by morphology (Figure 6a). In addition, injection of a missense MO into an in-cross of *fras1*$^{+/tm95b}$ fish (n=389 (308=wt, 81=mut)) had no effect on the severity of the caudal fin blistering phenotype (Figure 6a). Injection of *vwa2* MO into an in-cross of *fras1*$^{+/tm95b}$ fish (n=500 (400=wt, 100=mut)), however, resulted in a more severe phenotype, to a comparable level to that of null *fras1*$^{te262/te262}$ fish (Figure 6a). Representative morphologies of the caudal fin at 34 hpf for each condition are shown in Figure 6b. Analysis of Fras1 expression revealed high levels in the myosepta and fin of wild-type fish, reduced levels in uninjected and missense MO injected *fras1*$^{tm95b/tm95b}$ fish and a complete absence in *fras1*$^{te262/te262}$ fish and *fras1*$^{tm95b/tm95b}$ fish injected with *vwa2* MO, corresponding to the severity of the phenotype (Figure 6b). Laminin levels were consistent under all conditions (Figure 6b).

Discussion

FS is a heterogeneous disorder affecting the development of the skin, eyes, digits and kidneys. Although mutations in *FRAS1*, *FREM2* and *GRIP1* have been identified in approximately 95% of all FS patients, additional genetic contributions to this disorder remain likely. The highly variable inter- and intra-familial phenotypic severity of FS also suggests the presence of genetic

modifiers. In this study, we have demonstrated that *vwa2*, a gene encoding AMACO, a BM associated extracellular protein containing three von Willebrand factor A (VWA) domains, contributes to the Fraser complex in zebrafish and mice.

We could show that AMACO protein is completely absent in zebrafish and mouse mutants lacking Fras1, suggesting that Fras1 is crucial for the deposition or stabilization of AMACO. The *vwa2* mRNA expression level in Fras1 mutant zebrafish is, in contrast, completely normal (Suppl. 1) suggesting specific protein stabilization. TEM further supports a direct interaction, as AMACO and Fras1 co-localize at a distance that is consistent with direct binding in islands beneath the lamina densa. Unfortunately, a comprehensive study of the interaction between AMACO and Fras1 was hampered by the fact that the ectodomain, the VWC domains and the unique domain of Fras1 could not be recombinantly expressed in sufficient amounts. However, AMACO fragments covering the whole sequence were expressed and surface plasmon resonance spectroscopy revealed direct binding between AMACO P2 and the CSPG domains of Fras1.

Furthermore, we could demonstrate that knockdown of AMACO, which alone results in no morphological defects, can increase the phenotypic severity in hypomorphic Fras1 zebrafish. Upon AMACO knockdown the hypomorphic fish resemble the complete Fras1 knockout suggesting that, in addition to the requirement of Fras1 for AMACO deposition or stabilization, AMACO can stabilize Fras1. Reciprocal stabilization of Fras1, Frem1, Frem2 and possibly Frem3 has been suggested in mouse and zebrafish (Kiyozumi *et al.*, 2006; Carney *et al.*, 2010), whereas zebrafish Hmcn1, despite its co-expression with the FS genes and the similar phenotype of *hmcn1* and *fras1* mutants, is dispensable for Fras1 stabilization (Carney *et al.*, 2010). So, although loss of AMACO alone does not cause a tissue integrity phenotype, our results

demonstrate that AMACO can also stabilize Fras1 at the BM, potentially in a redundant manner with other Fraser complex proteins.

We currently do not know the nature of these potential redundant factors. For Frem2, the Fras1-stabilizing effect was only revealed upon concomitant knockdown of the three closely related proteins, Frem2a, Frem2b and Frem3 (Carney *et al.*, 2010). However, AMACO, although being a member of the VWA domain containing protein superfamily, does not belong to a distinct subfamily such as the matrilins or VWA domain containing collagens. Also, no direct AMACO paralogue has been annotated in the zebrafish genome. Therefore, it seems more likely that AMACO acts in partial functional redundancy with a more distantly related VWA protein. Nevertheless, the essential character of AMACO becomes apparent when Fras1 function is compromised. This indicates that interactions between several members of the Fraser complex are required for stabilization beneath the BM, with AMACO's function to support this structural complex becoming vital when the multi-protein structure is compromised by reduced levels or activities of other components. Due to these particular genetic features of AMACO and its physical involvement in the Fraser complex both in zebrafish and mouse, *VWA2* represents an interesting candidate for human mutation analysis in multigenic scenarios, possibly mediating a genetic predisposition for Fraser syndrome aetiology.

Materials & Methods

Zebrafish husbandry

Embryos were obtained from natural crosses and staged according to Kimmel *et al.*, 1995. The mutant alleles *pif*^{te262} (*fras1*), *pif*^{tm95} (*fras1*), *nel*^{tq207} (*hmcn1*), *bla*^{ta90} (*frem2a*) and *rfl*^{tc280b} (*frem1a*) have been described previously (Carney *et al.*, 2010).

Antisense morpholino knockdown

Morpholino antisense oligonucleotides (Supplement) were designed by and obtained from Gene-Tools (Philomath, OR) and dissolved in distilled water to 1 mM stock solutions. Two different morpholinos covering the ATG translation start codon and the 5' UTR of *vwa2* were used, both resulting in translational inhibition. A five-mismatch morpholino was used as negative control. For injection, stocks were diluted to 0.1 mM in Danieau's buffer and phenol red (Nasevicius and Ekker, 2000). 0.5 nl of MO solution was injected into embryos at the 1–4 cell stage using glass needles pulled on a Sutter needle puller and a Nanoject injection apparatus (World Precision Instruments).

Mouse lines

E14.5 mouse embryos, generated from an in-cross of *Fras1*$^{+/bl}$ mice and fixed in 4% paraformaldehyde (PFA), were obtained from Peter Scambler (UCL, London, UK).

Tissue-labeling procedures

For whole-mount immunofluorescence analysis zebrafish were fixed in 4% PFA overnight at 4°C and washed with 1x PBS. Fish were then washed for several hours in dH_20, blocked in 10% fetal calf serum (FCS) in 1x PBS, 0.5% Triton-X, incubated in primary antibody in 10% FCS overnight at 4°C, washed extensively in 1x PBS, 0.5% Triton-X, incubated overnight in secondary antibody in 10% FCS at 4°C, washed extensively in 1xPBS, 0.5% Triton-X and re-fixed in 4% PFA. For immunofluorescence analysis on sections, tissue was dehydrated in a graded series of alcohols, cleared in Roti-Histol (Carl Roth) and embedded in paraffin wax. Immunofluorescence analysis was performed using standard protocols. Primary antibodies used were: rabbit anti-zebrafish AMACO (Gebauer *et al.,* 2010), rabbit anti-zebrafish Fras1 (Carney *et al.*, 2010), rabbit anti-mouse AMACO (Gebauer *et al.*, 2009), and rabbit anti-laminin (Sigma Aldrich, L9393). Images were captured on a Zeiss Axiophot, Zeiss Apotome, Zeiss Confocal (LSM710 META) or Leica M165 FC compound microscope.

For whole-mount alcian blue stainings, the embryos were washed in phosphate buffered saline and incubated in 0.1 mg/ml alcian blue in ethanol/acetic acid (4:1) for 2-6 h at 37°C. After clearing overnight by digestion with 50 mg/ml trypsin in 30% sodium tetraborate in water, the specimens were destained in 1% KOH/glycerol, flat-mounted between a slide and a coverslip and photographed using a Zeiss Axiophot microscope equipped with a Nikon digital camera. Whole-mount *in situ* hybridization was performed as previously described (Gebauer *et al*., 2010) and photographed using a Zeiss Axiophot microscope equipped with a Nikon digital camera.

Expression of full length AMACO and Fras1 fragments

Mouse cDNA fragments were generated by RT-PCR and cloned with 5'-terminal NheI and 3'-terminal NotI restriction sites using oligonucleotide primers (Supplemental Table). The amplified PCR products were inserted into a modified pCEP-Pu vector containing an N-terminal BM-40 signal peptide (Kohfeldt, 1997) followed by an N-terminal One-STrEP-tag (IBA GmbH) upstream of the restriction sites. The expression constructs were transfected into 293 EBNA cells with FuGENE HD (Roche) according to the manufacturer's instructions. The cells were cultured in the presence of 10% FCS prior to harvest of cells and cell culture supernatant. After filtration and centrifugation of recombinant protein-containing supernatants for 1 h at 10,000 × g, these supernatant were applied to a Streptactin column (1.5 ml; IBA GmbH) and eluted with 2.5 mM desthiobiotin, 150mM NaCl, 100 mM Tris-HCl, pH 8.0.

Fras1 antibody production

Purified mouse Fras1 CSPG was used for guinea pig immunization. The antiserum was purified by affinity chromatography on a column with antigen coupled to CNBr-activated Sepharose (GE Healthcare). Specific antibodies were eluted with 0.1 M glycine, pH 2.5, and the eluate was neutralized with 1 M Tris-HCl, pH 8.8. Specificity was tested by western blot (Suppl. 2). The antibody was only used for immunoelectron microscopy.

Surface plasmon resonance binding assays

Binding analyses were performed using a BIAcore2000 (GE Healthcare). All proteins were from mouse. Expression and purification of AMACO fragments has been described earlier (Gebauer et al., 2009) and purity of the proteins is documented in (Suppl. 3). Fras1 CSPG (2200 RUs), AMACO full-length (2300 RUs), AMACO P1 (2500 RUs), AMACO P2 (2400 RUs), and AMACO P3 (2500 RUs) were covalently coupled to carboxymethyldextran hydrogel 500M sensor chips (XanTec, Düsseldorf, Germany) using the amine coupling kit (GE Healthcare). Binding assays were performed at 25°C in 10 mM Hepes buffer, pH 7.4, containing 0.15 M NaCl, 3 mM EDTA, and 0.005% (v/v) P20 surfactant (HBS-EP buffer). Omission of EDTA and addition of 1mM $MgCl_2$ and $CaCl_2$ did not result in any change of binding events. Equilibrium dissociation constants (K_D) were then calculated as the ratio k_d/k_a. Kinetic constants were calculated by nonlinear fitting of association and dissociation curves (BIAevaluation 4.1 software).

Protein extraction and western blot

For protein extracts, 32 hpf wild type and morphant zebrafish larvae (50 each) were homogenized in 500µl 150mM NaCl, 2mM EDTA, 1% Nonidet P-40 and 50mM Tris, pH 7.4, put on ice for 15 min, 1/3 volume of 4x SDS sample buffer (8% (w/v) SDS, 40% (v/v) glycerol, 0.2% (w/v) bromphenol blue, 250mM Tris-HCl, pH 6.8) was added, the samples were boiled for 5 min, centrifuged for 10 min. and subjected to 4-12% (w/v) SDS PAGE. Proteins were transferred to a nitrocellulose membrane and detected using polyclonal antibodies diluted in TBS/5% milk powder. Bands were detected by chemoluminescence immunoassay using a peroxidase-conjugated swine anti rabbit secondary antibody (Dako). Image J was used for quantification of bands.

Electron microscopy

Wild type and morphant zebrafish larvae 48 hpf were anesthetized with 0.08% Tricaine, transferred into 6% glutaraldehyde in 0.1 M cacodylate buffer, pH 7.2, for immersion fixation and stored in this solution for 3 days at 4°C. Then the larvae were rinsed 2x 15 min in 0.1 M cacodylate buffer, pH 7.2, postfixed 120 min with 1% OsO_4 in 0.1 M cacodylate buffer, pH 7.2, at room temperature in the dark, rinsed again, dehydrated with acetone and embedded in araldite CY212 (Durcupan ACM, Fluka). Ultrathin sections were cut at grey interference colour (25-30 nm) with a 35°-diamond knife (Diatome) on an Ultracut E (Leica), stretched with chloroform vapour, mounted on 200 mesh copper grids (5 μm bar thickness) and contrasted 10 min with saturated (2%) uranyl acetate in 70% ethanol and 5 min with 0.2% aqueous lead citrate, pH 11.8. Microscopy was performed with a Zeiss EM109 (80 kV, 500 μm condenser 1 aperture, 200 μm condenser 2 aperture, 30 μm objective aperture) equipped with a temperature-stabilized wide angle YAC-CCD camera at the side entry port (1024x1024 pixel, 12-bit greyscale/pixel; info@trs-system.de). Magnification was calibrated with a cross grating replica (2160 lines/mm, d = 0.463 μm).

Immunoelectron microscopy

Newborn mouse skin was carefully sliced into 1 mm cubes, all including epithelium and dermis. Tissues were immersed in a combination of affinity purified rabbit AMACO-P3 antibody (Gebauer et al., 2009) or collagen VII antibody (Lunstrum et al., 1986) with guinea pig Fras1 CSPG antibody (Suppl. 2) in Dulbecco's Modified Eagle Media (DMEM) at a ratio of 1:1:4

overnight at 4°C. Tissues were washed in DMEM for 4 hours at 4°C and then immersed in a combination of goat anti-rabbit 10-nm and goat anti-guinea pig 6-nm colloidal gold conjugates in DMEM at a ratio of 1:1:3 overnight at 4°C. The tissues were then rinsed extensively in DMEM, fixed in 1.5% glutaraldehyde/1.5% paraformaldehyde containing 0.5% tannic acid, post-fixed in 1% OsO_4, then dehydrated and embedded in Spurr's epoxy resin. Tissue was oriented so that cross sections of the dermal-epidermal junction would be obtained. Ultrathin sections were contrasted with uranyl acetate and lead citrate and examined using a FEI Tecnai G20 TEM.

Conflict of Interest

The authors state no conflict of interest.

Acknowledgments

Excellent technical assistance from Evelin Fahle and Petra Müller is gratefully acknowledged. We are very grateful to Peter Scambler for Fras1 (bleb) mutant mice. Work in the laboratories of RW and MP was funded by the Deutsche Forschungsgemeinschaft (WA1338/2-6 and SFB829/B2), work in the laboratory of GS by the Deutsche Forschungsgemeinschaft (SFB829/B12), work in the laboratory of MH by the Deutsche Forschungsgemeinschaft (SFB829/A9), the European Union (Seventh Framework Program, Integrated Project ZF-HEALTH, EC Grant Agreement HEALTH-F4-2010-242048), the US National Institute of General Medical Sciences (GM63904), and an EMBO long-term postdoctoral fellowship to RR. JMG was a member of the International Graduate School in Genetics and Functional Genomics at the University of Cologne.

References

Alazami AM, Shaheen R, Alzahrani F, *et al.* (2009). FREM1 mutations cause bifid nose, renal agenesis, and anorectal malformations syndrome. *Am J Hum Genet*. 85:414-18.

Carney TJ, Feitosa NM, Sonntag C, *et al.* (2010). Genetic analysis of fin development in zebrafish identifies furin and hemicentin1 as potential novel fraser syndrome disease genes. *PLoS Genet* 6:e1000907.

Dalezios Y, Papasozomenos B, Petrou P, *et al.* (2007). Ultrastructural localization of Fras1 in the sublamina densa of embryonic epithelial basement membranes. *Arch Dermatol Res* 299:337-43.

Drummond IA (2005). Kidney development and disease in the zebrafish. *J Am Soc Nephrol* 16:299-304.

Gebauer JM, Karlsen KR, Neiss WF, *et al.* (2010). Expression of the AMACO (VWA2 protein) ortholog in zebrafish. *Gene Expr Patterns* 10:53-59.

Gebauer JM, Keene DR, Olsen BR, et al (2009). Mouse AMACO, a kidney and skin basement membrane associated molecule that mediates RGD-dependent cell attachment. *Matrix Biol* 28:456-62.

Gebauer, JM, Müller, S, Hanisch, FG, *et al.* (2008). O-glucosylation and O-fucosylation occur together in close proximity on the first epidermal growth factor repeat of AMACO (VWA2 protein). *J Biol Chem* 283:17846-54.

Jadeja S, Smyth I, Pitera JE, *et al.* (2005). Identification of a new gene mutated in Fraser syndrome and mouse myelencephalic blebs. *Nat Genet* 37: 520-25.

Kimmel CB, Ballard WW, Kimmel SR, *et al.* (1995). Stages of embryonic development of the zebrafish. *Dev Dyn* 203:253–310.

Kiyozumi D, Sugimoto N, Nakano I, *et al.* (2007). Frem3, a member of the 12 CSPG repeats-containing extracellular matrix protein family, is a basement membrane protein with tissue distribution patterns distinct from those of Fras1, Frem2, and QBRICK/Frem1. *Matrix Biol* 26:456-62

Kiyozumi D, Sugimoto N and Sekiguchi K. (2006) Breakdown of the reciprocal stabilization of QBRICK/Frem1, Fras1, and Frem2 at the basement membrane provokes Fraser syndrome-like defects. *Proc Natl Acad Sci U S A*. 103(32):11981-6.

Kohfeldt E, Maurer P, Vannahme C *et al.* (1997). Properties of the extracellular calcium binding module of the proteoglycan testican. *FEBS Lett*. 414:557-61.

Long J, Wei Z, Feng W, *et al.* (2008). Supramodular nature of GRIP1 revealed by the structure of its PDZ12 tandem in complex with the carboxyl tail of Fras1. *J Mol Biol* 375:1457-68.

McGregor L, Makela V, Darling SM, *et al.* (2003). Fraser syndrome and mouse blebbed phenotype caused by mutations in FRAS1/Fras1 encoding a putative extracellular matrix protein. *Nat Genet* 34:203-8.

Nasevicius A, and Ekker SC (2000) Effective targeted gene 'knockdown' in zebrafish. *Nat Genet* 26:216–220.

Petrou P, Chiotaki R, Dalezios Y, *et al.* (2007a). Overlapping and divergent localization of Frem1 and Fras1 and its functional implications during mouse embryonic development. *Exp Cell Res* 313:910-20.

Petrou P, Pavlakis E, Dalezios Y, *et al.* (2007b). Basement membrane localization of Frem3 is independent of the Fras1/Frem1/Frem2 protein complex within the sublamina densa. *Matrix Biol* 26:652-58.

Sengle G, Kobbe B, Mörgelin M, *et al.* (2003). Identification and characterization of AMACO, a new member of the von Willebrand factor A-like domain protein superfamily with a regulated expression in the kidney. *J Biol Chem* 278:50240-9.

Slavotinek AM, Baranzini SE, Schanze D, *et al.* (2011). Manitoba-oculo-tricho-anal (MOTA) syndrome is caused by mutations in FREM1. *J Med Genet* 48:375-82.

Slavotinek AM and Tifft CJ. (2002) Fraser syndrome and cryptophthalmos: review of the diagnostic criteria and evidence for phenotypic modules in complex malformation syndromes. *J Med Genet*. 39:623-33.

Takamiya K, Kostourou V, Adams S, *et al.* (2004). A direct functional link between the multi-PDZ domain protein GRIP1 and the Fraser syndrome protein Fras1. *Nat Genet* 36:172-77.

Talbot JC, Walker MB, Carney TJ, *et al.* (2012). fras1 shapes endodermal pouch 1 and stabilizes zebrafish pharyngeal skeletal development. *Development*. 139:2804-13.

van Haelst MM, Maiburg M, Baujat G, *et al.* (2008). Molecular study of 33 families with Fraser syndrome new data and mutation review. *Am J Med Genet A* 146A:2252-57.

Vogel MJ, van Zon P, Brueton L, *et al.* (2012). Mutations in GRIP1 cause Fraser syndrome. *J Med Genet* 49:303-6.

Vrontou S, Petrou P, Meyer BI, *et al.* (2003). Fras1 deficiency results in cryptophthalmos, renal agenesis and blebbed phenotype in mice. *Nat Genet* 34:209-14.

Figure Legends

Figure 1 - AMACO expression is affected in zebrafish models of Fraser syndrome. Immunofluorescence analysis of whole-mount zebrafish at 32 hpf reveals that (**a**) AMACO is strongly expressed in the myosepta and developing caudal fin of wild-type zebrafish, highly similar to the expression of Fras1 (inset). (**b,c**) By contrast, AMACO is completely absent from a zebrafish Fras1 null allele (*fras1*$^{te262/te262}$) (**b**), and partially lost from a hypomorphic Fras1 allele (*fras1*$^{tm95b/tm95b}$) which exhibits some residual Fras1 expression (**c**). (**d-f**) AMACO expression is normal in null alleles for Frem2a (*frem2a*$^{ta90/ta90}$; **d**), Frem1a (*frem1a*$^{tc280b/tc280b}$; **e**) and Hemicentin1 (*hmcn1*$^{tq207/tq207}$; **f**). Expression of Fras1 is also normal in each of these alleles (inset in **d-f**). Scale bar = 500 μm. (**g,h**) Quantitative AMACO immunoblot analysis and quantification in the zebrafish mutant strains shown in a-f. In each case a pool of 50 fish of a given phenotype was extracted. In g, Ponceau loading control is given below. Antibodies are against zebrafish proteins (Gebauer et al., 2010; Carney et al. 2010).

Figure 2 - AMACO expression is lost from Fras1 mutant mice. (**a-f**) Immunofluorescence analysis of the epidermis of E14.5 wild type (**a,d**), *Fras1*$^{+/bl}$ (**b,e**) and *Fras1*$^{bl/bl}$ (**c,f**) littermates reveals a complete loss of AMACO expression from the basement membrane of *Fras1*$^{bl/bl}$ mice (**c**), whereas laminin expression is normal (**f**). (**g-l**) Similar analysis of other regions demonstrates the loss of AMACO from a blister over the eye of an E14.5 *Fras1*$^{bl/bl}$ embryo (**g**) whereas laminin expression was still observed under the detached epidermis (**j**). Strong expression of AMACO was observed surrounding the developing tooth germs of E14.5 wild-type mice (**h**) but was completely lost from a *Fras1*$^{bl/bl}$ littermate (**i**) despite laminin being normal (**k,l**). Scale bars = 50

µm. For generation and characterization of the mouse AMACO-P3 antibody see Gebauer *et al*., 2009.

Figure 3 - Fras1 and AMACO co-localize at the basement membrane. (a-c) For immuno-EM analysis, newborn mouse skin was immunolabeled enbloc with antibodies directed against mouse AMACO-P3, human collagen VII and mouse Fras1-CSPG. Secondary antibodies conjugated to gold particles of different size (Fras1: 6 nm; AMACO and collagen VII: 10 nm) were detected at anchoring plaques below the lamina densa (LD, black arrowheads). Often anchoring fibrils (AF, open arrowheads) are seen to intersect the anchoring plaques (AP). Collagen VII (arrows) and Fras1 often occur at opposite sides of anchoring plaques (**c**). (**a and c**) shows an overview and (**b**) shows selected anchoring plaques. The scale bar corresponds to 100 nm in (**a** and **c**) and 50 nm in (**b**).

Figure 4 – AMACO and Fras1 interact directly. (**a**) Domain structures of Fras1 and AMACO. (S) signal peptide, (TM) transmembrane domain, the arrow indicates the furin cleavage site. (**b, c**) Surface plasmon resonance sensorgrams showing binding of different concentrations of soluble analytes to Fras1 CSPG (**b**) and AMACO P2 (**c**) coupled onto a chip. Full-length AMACO interacts with Fras1 CSPG, as does the AMACO P2 fragment. AMACO P1 and AMACO P3 do not interact (**b**). In the reversed orientation Fras1 CSPG interacts with AMACO P2 (**c**). All proteins were from mouse.

Figure 5 - AMACO deficient zebrafish are phenotypically normal. (**a-d**) Injection of a *vwa2* specific morpholino has no effect on caudal fin development at 48 hpf (**b**) even though complete knockdown of the protein is observed (**d**). By contrast the levels of Fras1 in the developing fin of

vwa2 morphants are normal (inset in **d**). Antibodies were against zebrafish proteins (Gebauer *et al*., 2010; Carney *et al*. 2010). (**e,f**) TEM analysis at 48 hpf reveals no defect in the structure of the myosepta in *vwa2* morphants (**f**) when compared to wild-type controls (**e**). (**g,h**) Similarly, no abnormalities can be observed in the craniofacial cartilages or general morphology of *vwa2* morphants at 80 hpf (**h**). My = myosepta; Pq, palatoquadrate; Ch, ceratohyal; Ih, interhyal; Hm, hyomandibular; Sy, symplectic.

Figure 6 - *vwa2* knockdown in Fras1 hypomorphic zebrafish increases the severity of the phenotype. (**a**) Chart depicting the relative severity of the blistering phenotype of Fras1 zebrafish injected with a missense morpholino (5mm) or a *vwa2* specific MO. In all cases, mutant embryos were derived from heterozygous in-crosses, segregating in a normal Mendelian ratio. Only homozygotes are considered in the chart. Included are representative images of mild, moderate and severe blistering. Severe blistering was determined by a large number of caudal fin blisters (arrowheads) often extending further anterior within the dorsal region of the caudal fin. Associated extensive blistering of the caudal vein region was also observed (arrows). Moderate blistering involved fewer fin tip blisters of variable sizes and less although always some associated caudal vein blistering. Mild blistering was determined by a small number of fin tip blisters with no associated caudal vein blistering. Compare to **b** for a representative wild type fin. (**b**) Immunolocalization of Fras1 and laminin are also shown for each condition. The Fras-1 antibodies are specific for zebrafish (Carney *et al*. 2010).

Supplemental Table 1
Oligonucleotide sequences used for cDNA construction

cDNA construct	**name**	**forward primer (5'- 3')**	**name**	**reverse primer (5'- 3')**
AMACO full-length	BK625	CAATGCTAGCCTTCAG GAAGTGCATGTGAAC	BK626	CAATGCGGCCGCTTACTTG GCGGAGGACAGG
Fras1 ectodomain	BK569	CAATGCTAGCGCTTGT CTGTATCAGGGC	BK570	CAATGCGGCCGCCTACTTA TAGAGGGCATCTACTTTG
Fras1 VWC	BK569	CAATGCTAGCGCTTGT CTGTATCAGGGC	BK609	CAATGCGGCCGCCTATACT GGTGTGCAGTCTGG
Fras1 Furin	BK610	CAATGCTAGCGTACAC TGCCACCCAGAC	BK611	CAATGCGGCCGCCTAGTCA GTACAGTTTTCATTAGATG
Fras1 CSPG	BK612	CAATGCTAGCGACAAA ATGTACACTCCAAGTC	BK613	CAATGCGGCCGCCTACTCC TGGGTGAAGGTG
Fras1 CALX	BK614	CAATGCTAGCGAGCAT GTGAACTTGGG	BK615	CAATGCGGCCGCCTAAATG GGTGGCGCTG
Fras1 unique	BK616	CAATGCTAGCGTAGTC ACTCTTGCTGACTATG	BK570	CAATGCGGCCGCCTACTTA TAGAGGGCATCTACTTTG
vwa2 RT-PCR				
β-actin control				

Antisense morpholinos

zAMACOas1 5'-CGGCTGCTTGAAGACATTTTTGTGC-3'
zAMACOas2 5'-CTTAGTGACACCGCAGTCCTGTTTA-3'
zAMACOmis1* 5'-CGCCTGGTTGAACACAATTTTCTGC-3'

*Mismatches in the target sequence are underlined.

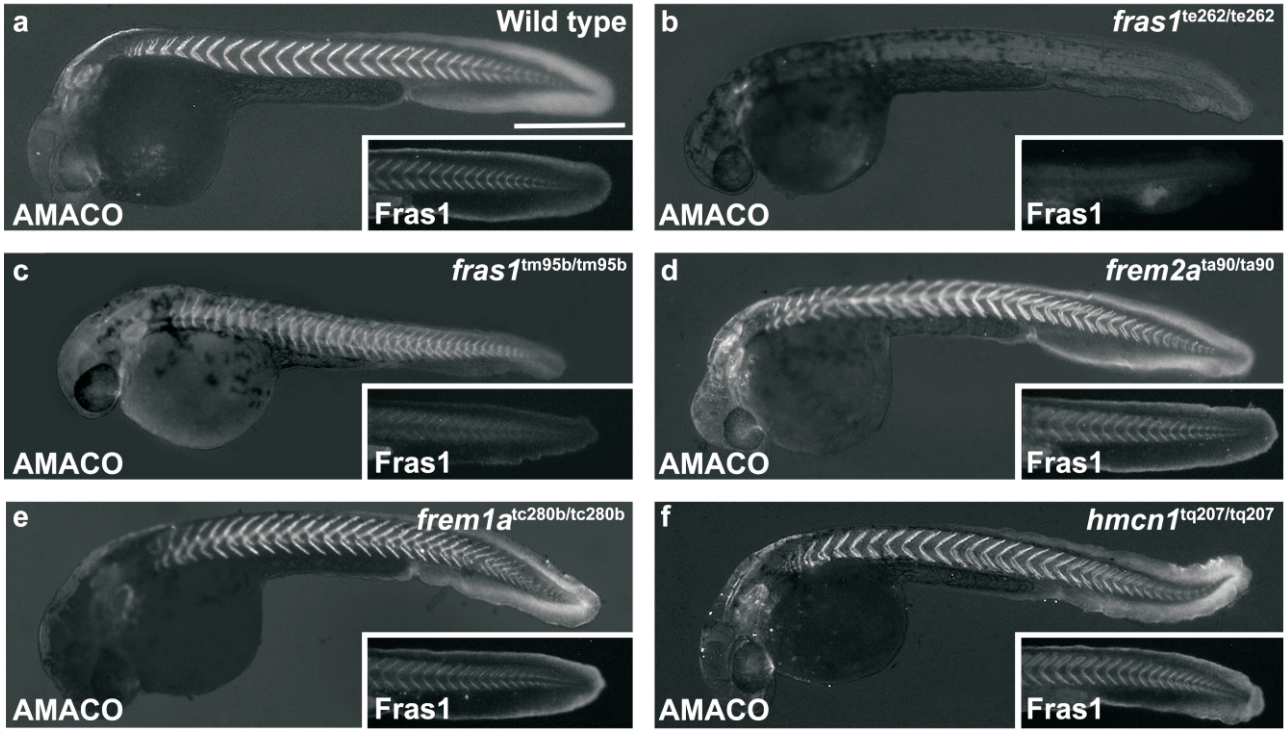
a
Wild type
AMACO
Fras1
b
fras1te262/te262
AMACO
Fras1
c
fras1tm95b/tm95b
AMACO
Fras1
d
frem2ata90/ta90
AMACO
Fras1
e
frem1atc280b/tc280b
AMACO
Fras1
f
hmcn1tq207/tq207
AMACO
Fras1

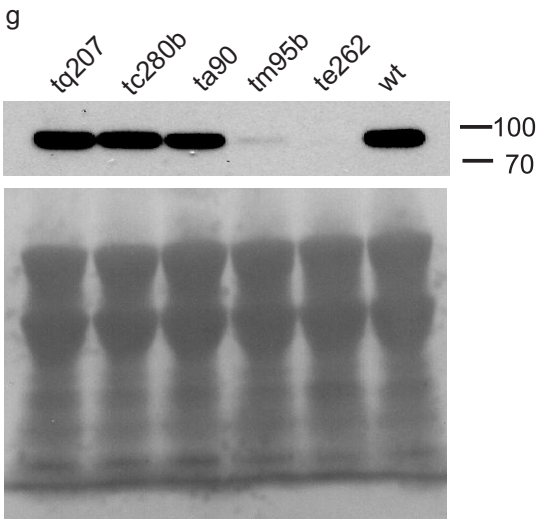
g
tq207
tc280b
ta90
tm95b
te262
wt
100
70

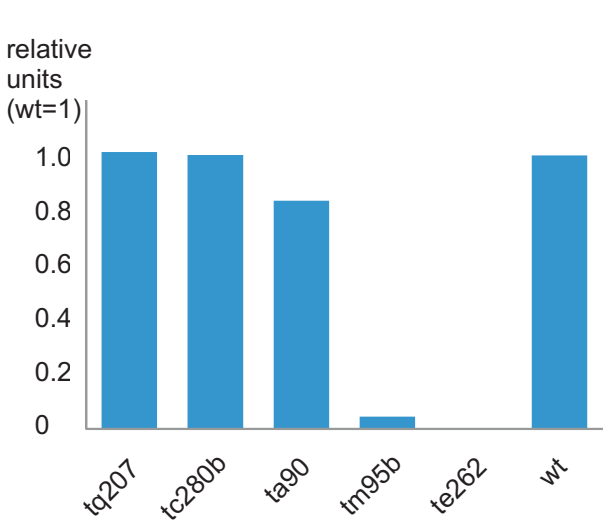
h
relative units (wt=1)
1.0
0.8
0.6
0.4
0.2
0
tq207
tc280b
ta90
tm95b
te262
wt

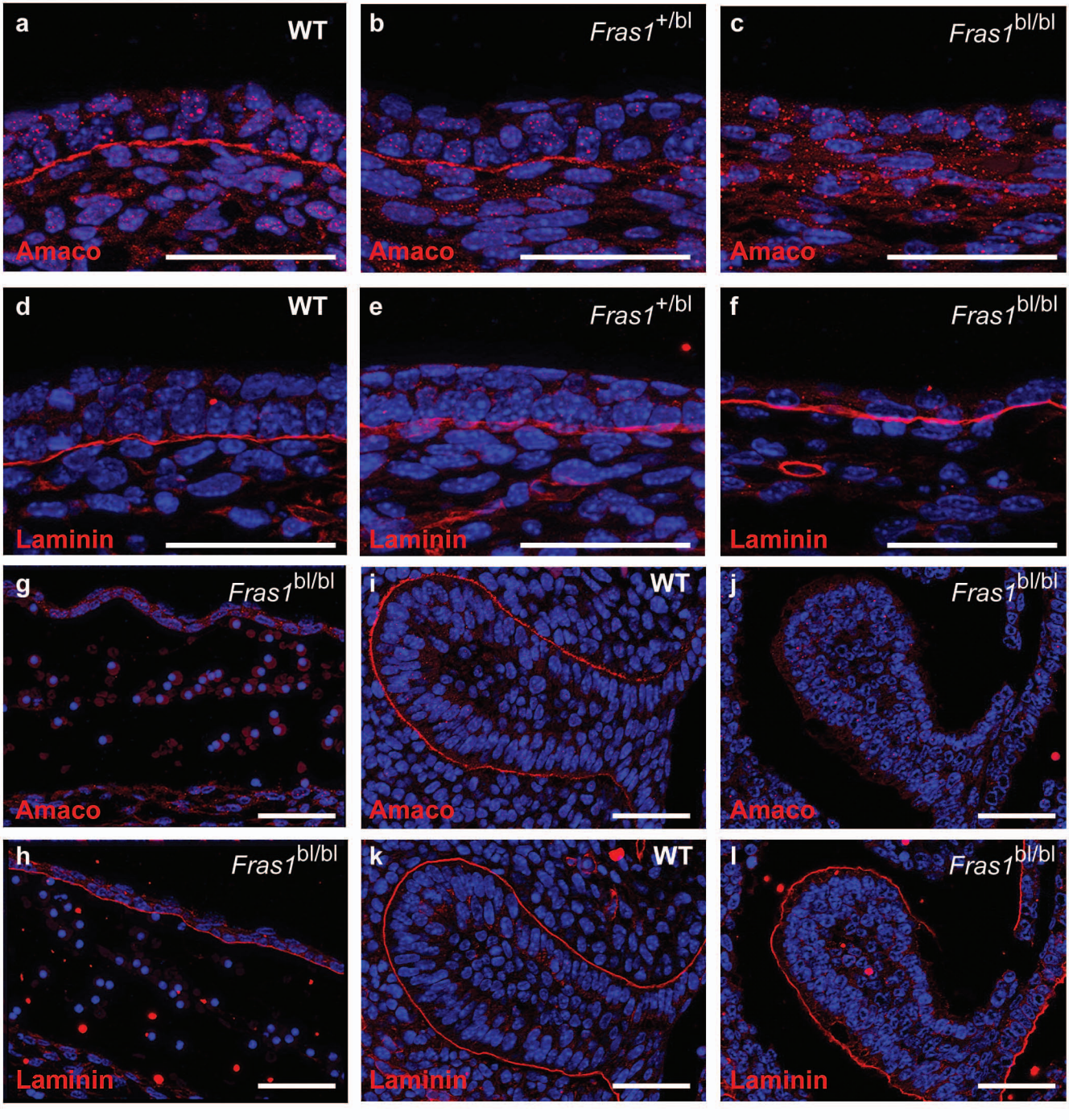
a
WT
Amaco
b
Fras1+/bl
Amaco
c
Fras1bl/bl
Amaco
d
WT
Laminin
e
Fras1+/bl
Laminin
f
Fras1bl/bl
Laminin
g
Fras1bl/bl
Amaco
i
WT
Amaco
j
Fras1bl/bl
Amaco
h
Fras1bl/bl
Laminin
k
WT
Laminin
l
Fras1bl/bl
Laminin

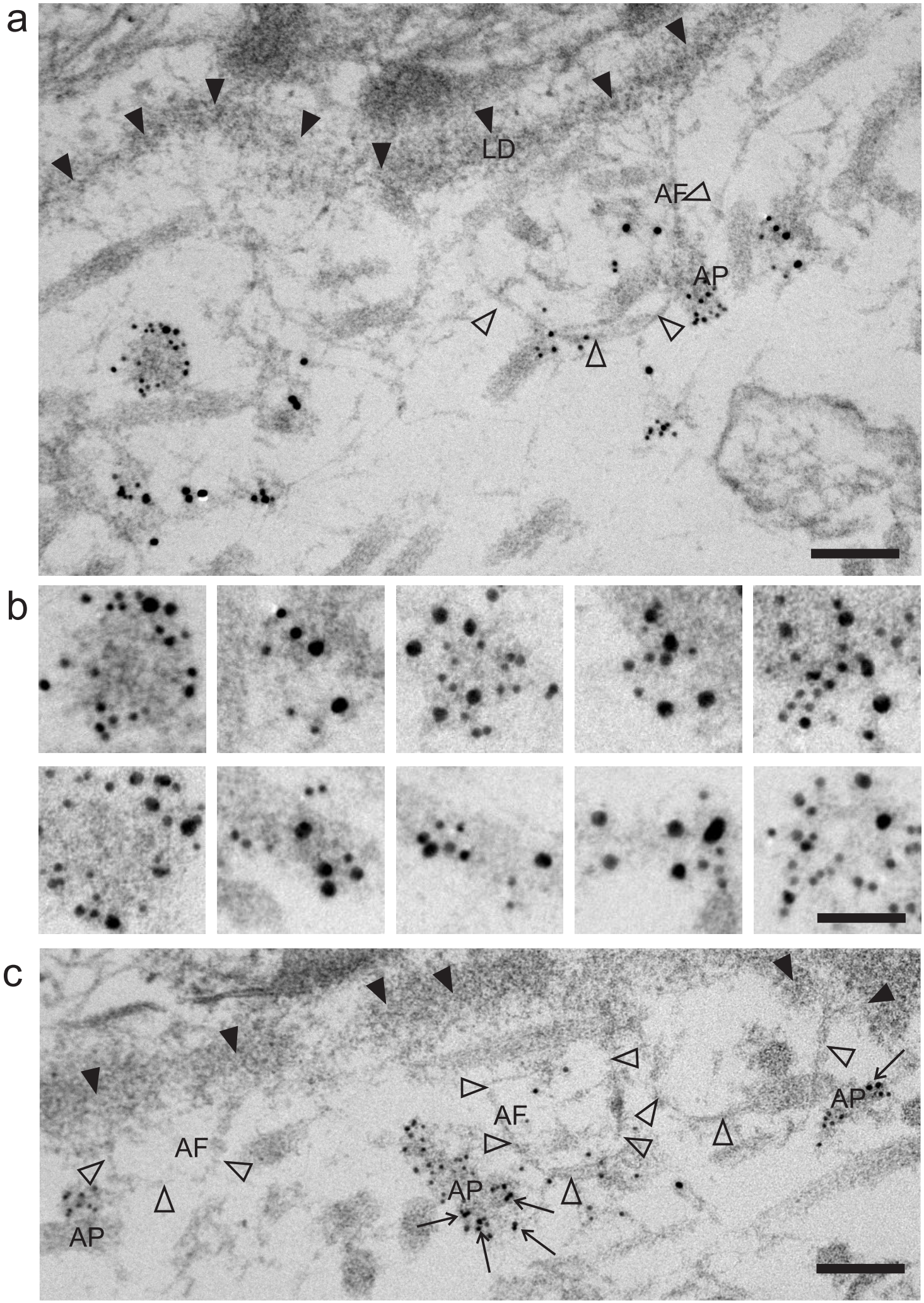
a
LD
AF
AP
b
c
AF
AF
AP
AP
AP

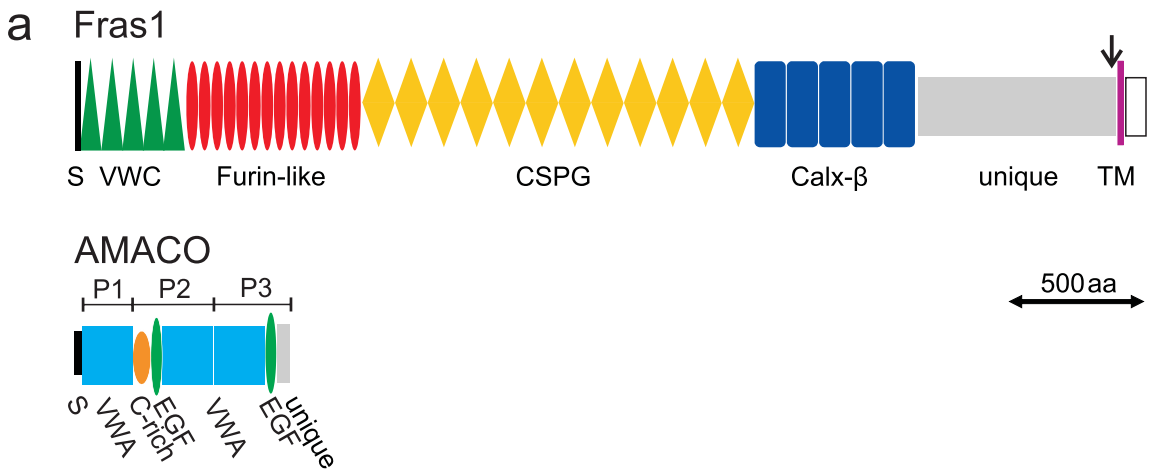
a
Fras1
S
VWC
Furin-like
CSPG
Calx-β
unique
TM
AMACO
P1
P2
P3
500 aa
S
VWA
C-rich
EGF
VWA
EGF
unique

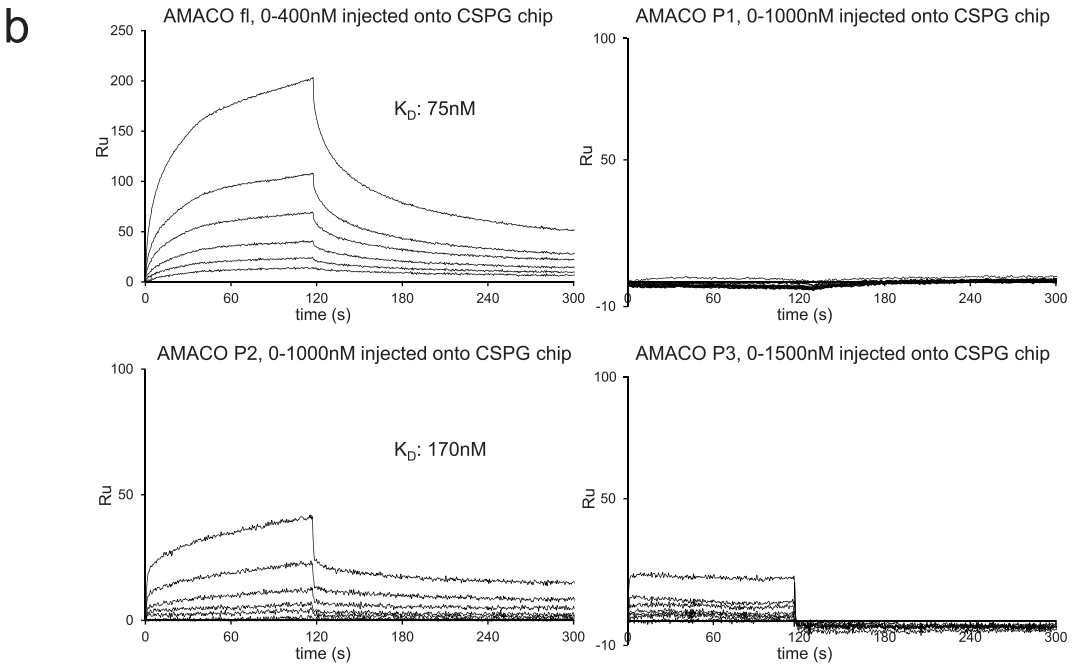
b
AMACO fl, 0-400nM injected onto CSPG chip
K_D: 75nM
AMACO P1, 0-1000nM injected onto CSPG chip
AMACO P2, 0-1000nM injected onto CSPG chip
K_D: 170nM
AMACO P3, 0-1500nM injected onto CSPG chip
Ru
time (s)

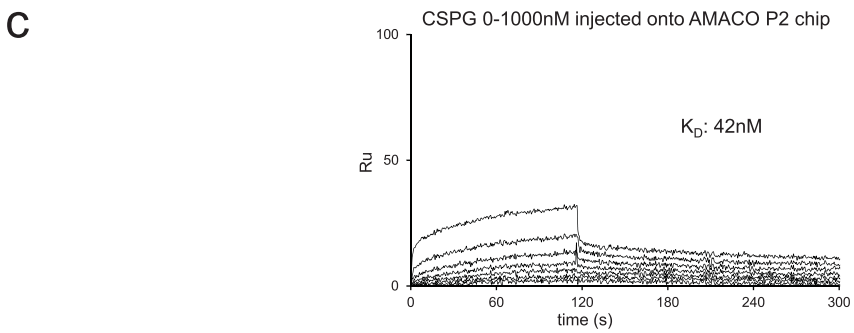
c
CSPG 0-1000nM injected onto AMACO P2 chip
K_D: 42nM
Ru
time (s)

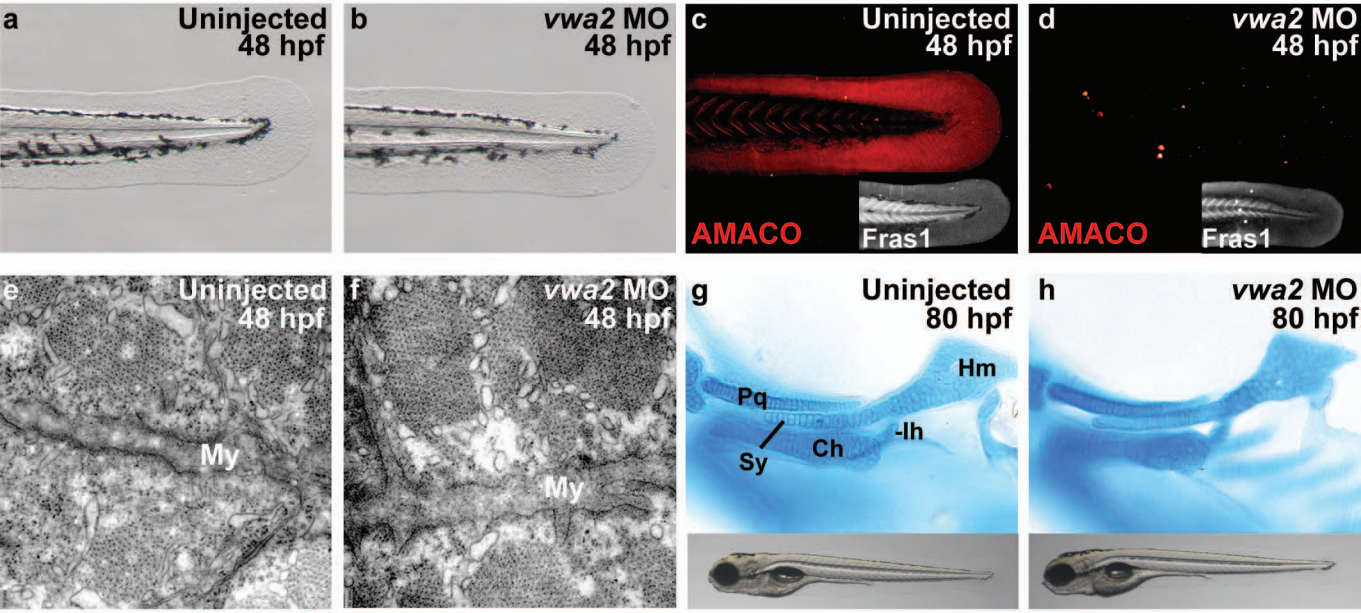
a
Uninjected
48 hpf
b
vwa2 MO
48 hpf
c
Uninjected
48 hpf
AMACO
Fras1
d
vwa2 MO
48 hpf
AMACO
Fras1
e
Uninjected
48 hpf
My
f
vwa2 MO
48 hpf
My
g
Uninjected
80 hpf
Hm
Pq
Sy
Ch
-Ih
h
vwa2 MO
80 hpf

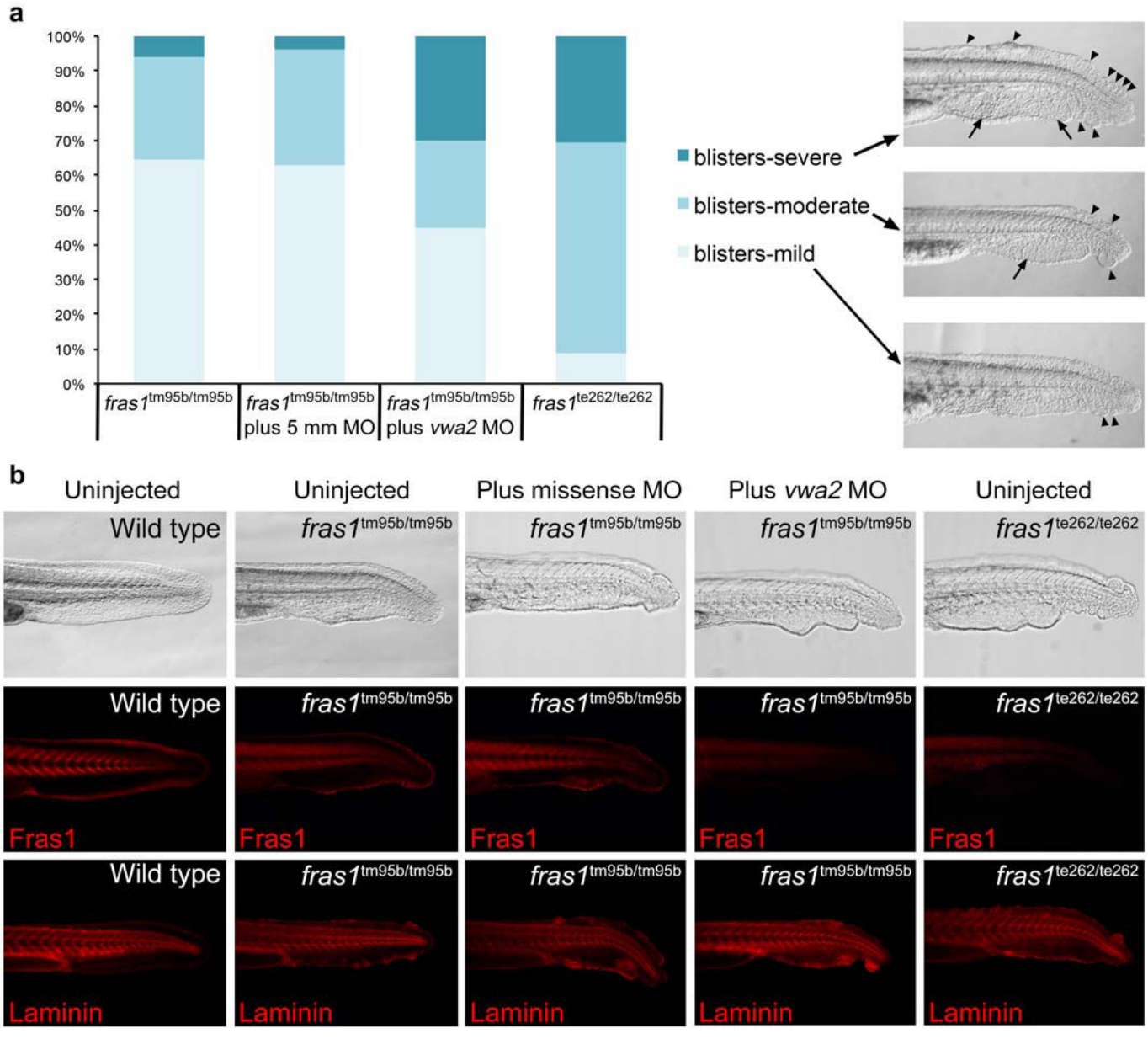
a
100%
90%
80%
70%
60%
50%
40%
30%
20%
10%
0%
fras1tm95b/tm95b
fras1tm95b/tm95b plus 5 mm MO
fras1tm95b/tm95b plus vwa2 MO
fras1te262/te262
blisters-severe
blisters-moderate
blisters-mild
b
Uninjected
Uninjected
Plus missense MO
Plus vwa2 MO
Uninjected
Wild type
fras1tm95b/tm95b
fras1tm95b/tm95b
fras1tm95b/tm95b
fras1te262/te262
Fras1
Laminin

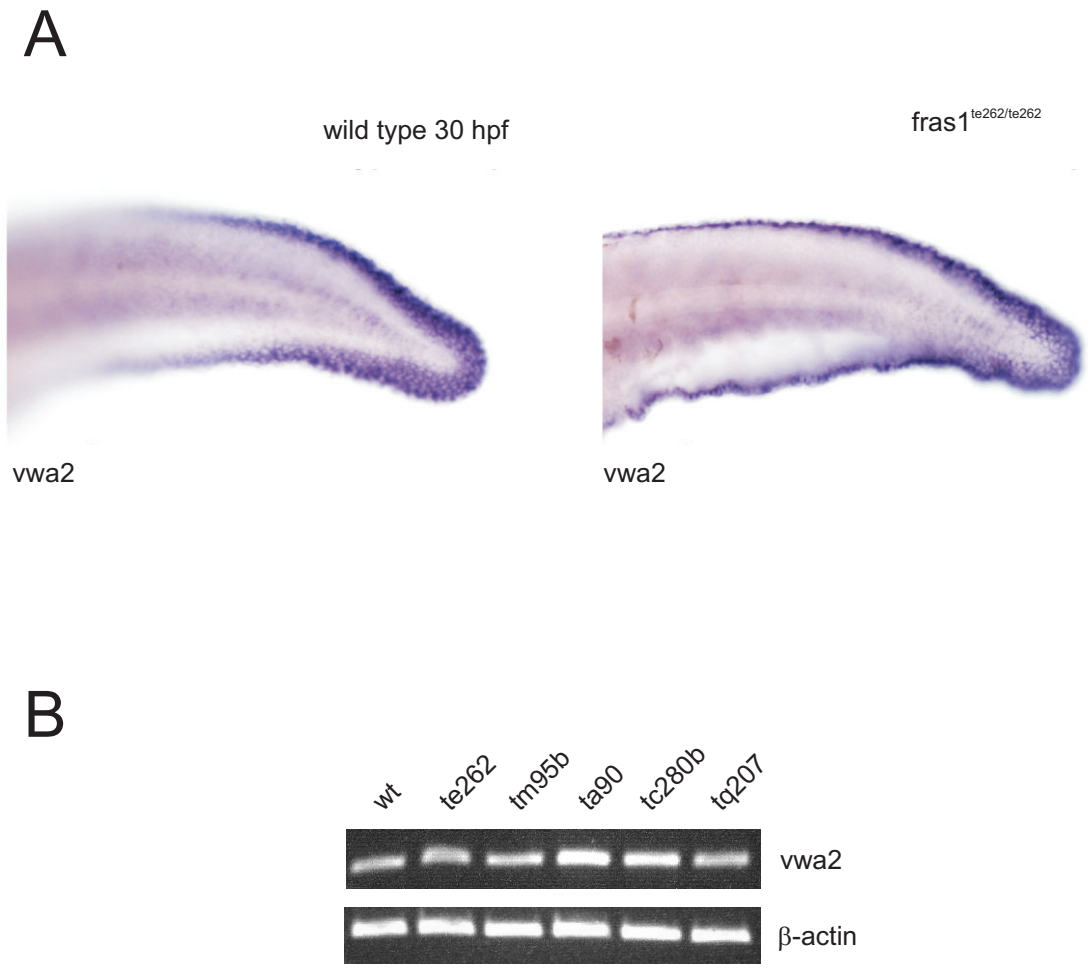

Supplemental figure 1. Normal expression of vwa2 in fras1 mutant fish. (A) In situ hybridization reveals comparable levels of vwa2 mRNA in the developing caudal fin of wild type and fras1te262/te262 null fish at 30 hpf. (B) RT-PCR reveals comparable levels of vwa2 mRNA in whole wild type and fras1 mutant fish. te262, fras1null ; tm95b, fras 1 hypomorph, ta90, frem1a mutant; tc280b, frem2a mutant; tq207, hmcn1. β-actin was used as control. RT-PCR was performed as previously described (Gebauer *et al*., 2010). The primers are given in Supplemental Table 1.

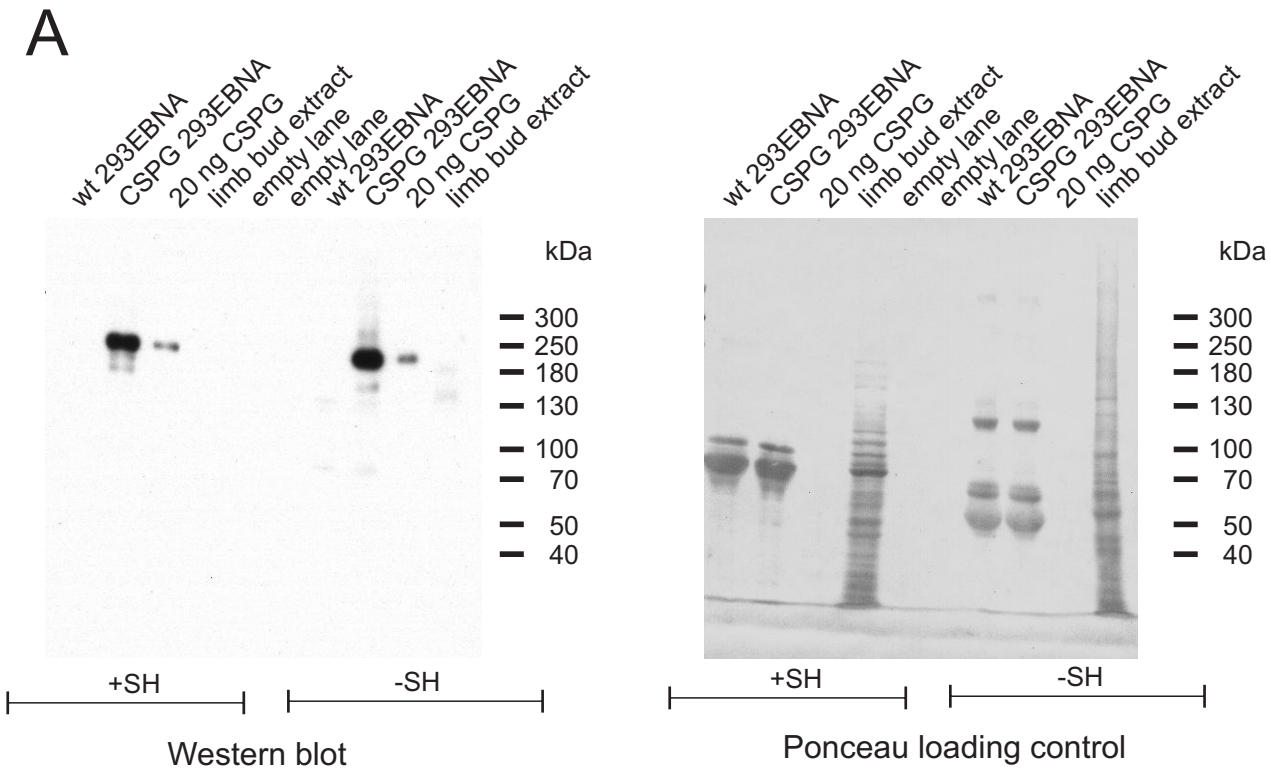

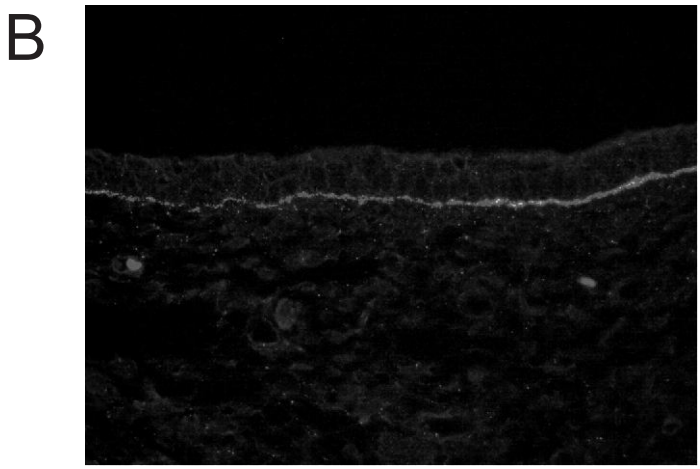

Supplemental figure 2 Specificity of the guinea pig Fras1 CSPG antibody. A, immunoblot analysis. Cell culture supernatants from wild-type 293EBNA cells (wt-293EBNA), from 293EBNA cells transfected with the Fras1 CSPG domain (CSPG 293EBNA), 20 ng of affinity purified Fras1 CSPG (20 ng CSPG) and a limb bud extract from 18.5-day- old mouse embryos were separated by reducing (+SH) and non-reducing (-SH) SDS-PAGE on 4-12% polyacrylamide gels and transferred to nitrocellulose. The blot was subsequently developed with the affinity-purified Fras1 CSPG antibody. On the right, Ponceau staining is shown to demonstrate protein load. Limb buds were extracted with TBS. B. Immunofluorescence staining. A paraffin-embedded section of skin from a 14.5 mouse embryo was stained with the affinity-purified guinea pig antibody directed against the murine Fras1 CSPG domains followed by incubation with Alexa 488 (red) coupled secondary antibodies. Fras1 is only detected in the basement membrane.

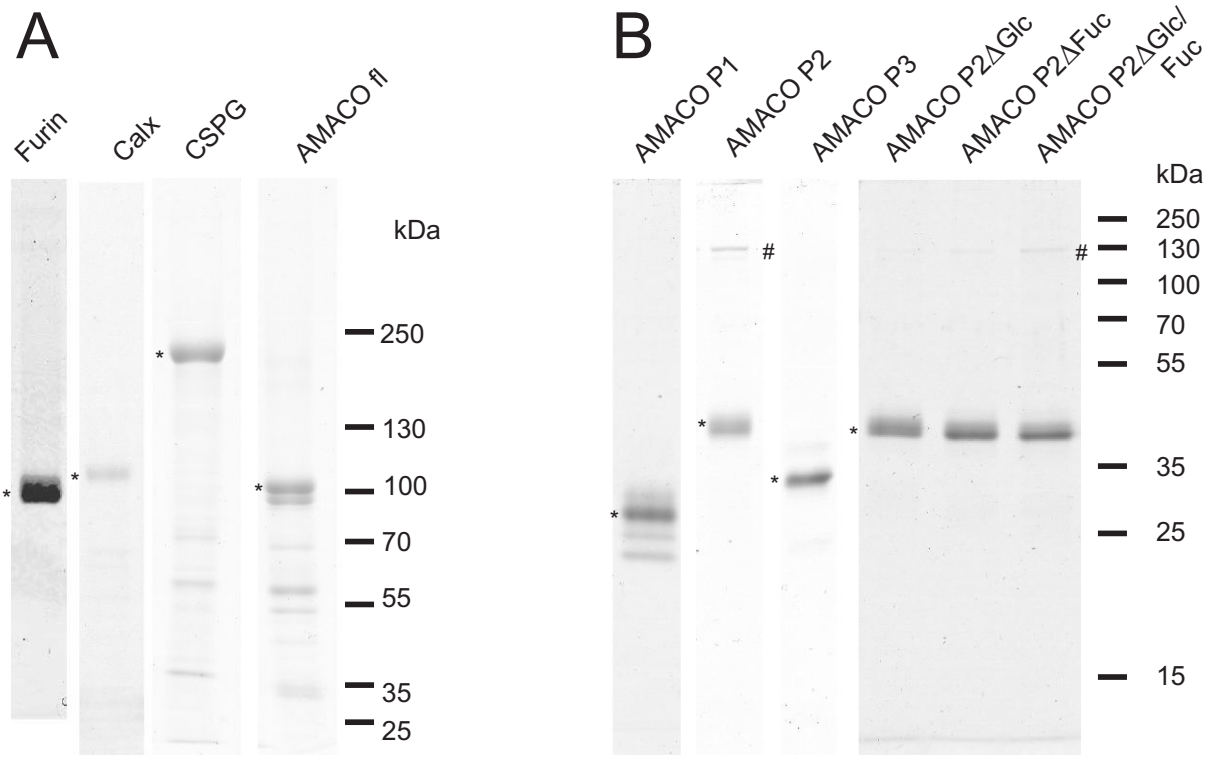

Supplemental figure 3. Recombinant expression of proteins used for SPR analysis. Affinity purified proteins were submitted to SDS-PAGE (4-12% polyacrylamide gels in (A) and 12% gels in (B)) under reducing conditions and stained with Coomassie brilliant blue. The Fras1 fragments CSPG, Furin and Calx and AMACO full-length (fl) carry a One-STrEP-tag, AMACO wild type fragments (P1–P3) and mutant AMACO-P2 lacking O-fucosylation and O-glucosylation sites (Δgluc, Δfuc, Δgluc/fuc) carry a 8X his tag. Bands of the expected size are marked by asteriscs. Lower migrating bands in CSPG, AMACO fl and AMACO P1 contain degradation products, the bands marked by # in the lanes for AMACO P2 contain calsyntenin 1.